DECAY OF LASER SIGNAL FLUCTUATIONS IN SNOWFALL WHEN USING NON-POINT RECEIVER

A.G. Borovoy, N.A. Vostretsov, A.F. Zhukov, R.Sh. Tsvyk, and V.P. Yakubov

Institute of Atmospheric Optics, Biberian Branch of the Russian Academy of Science, Tomsk
Tomsk State University
Received August 1, 1997

A dependence of a laser signal fluctuations dispersion on the path length was studied experimentally in narrow divergent beam in a snowfall under close atmospheric conditions provided that non-point receiver was used. The fluctuations were found in decay with the path length increase.

Fluctuations of the intensity of narrow laser beams during their propagation in snowfalls were considered by us in Refs. 1–5. In particular, three regimes of the intensity fluctuations for light propagated in precipitation were established, namely, regime of weak, saturated, and damping fluctuations. A point receiver was used in these experiments.

Of practical interest are the signal fluctuations when the size of the receiver exceeds the spatial radius of the intensity correlation resulting in an averaging over a receiving aperture. The regime of saturated fluctuations in a snowfall for the non-point receiver was examined by us experimentally in Refs. 3 and 4. The results of analogous experimental research of the regime of damping fluctuations are given in the present paper. Measurements were carried out at the Tomsk experimental site in winter 1997.

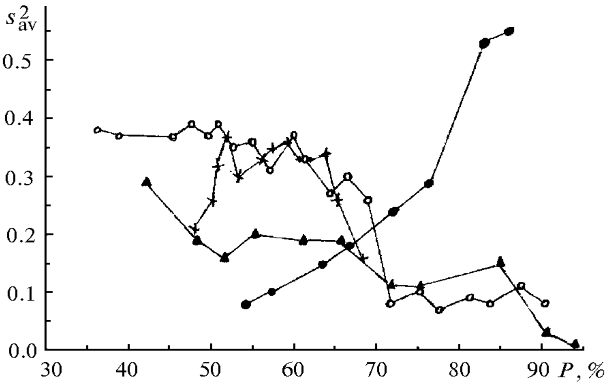

FIG. 1. Dependence of the averaging scintillation index (s^2_{av}) on the transparency (P) on the paths (2×100), 260, 520, 780 *and* 2048 m *long:* t = 260(▲), 520(○), 780(+), *and* 2048 (●).

To proceed to the regime of damping fluctuations a 2048-m path was equipped. Snowfalls with small sizes of snow flakes (maximum diameter 1–3 mm) were analyzed. The diameter of the receiver was equal to 3.1 mm^2, which provides the non-point receiver. The measurements of the scintillation index of the intensity fluctuations on the 2048-m path are shown in Fig. 1 by black circles. The scintillation index is defined by the following expression:

$$s^2 = (<I^2> - <I>^2)/<I>^2, \quad (1)$$

where I is the measurable signal and <...> denotes temporal averaging over a period of 20 s for their measurements. In contrast with Refs. 1–5, the transparency P experimentally measured on the path of length 2×100 m rather than the optical thickness of snowfall is plotted on the abscissa here.

The points snown in the figure are the results of averaging of the experimental data with a transparency step of 5%. Thus, different optical thicknesses correspond to different path lengths for the given value of P.

For comparation, the data from Ref. 4 for shorter paths are shown in the figure. As can be seen, the data obtained on the 2048-m path at first sight, exhibit other qualitative regularities. Indeed, with the increase of the snowfall intensity on paths 260 and 520 m long the scintillation index increases and fluctuations than saturate, whereas the path 780 m long the scintillation index for heavy snowfall enters the regime of damping fluctuations. In contrast, the scintillation index on the path 2048-m long decreases monotonically.

The qualitative difference of fluctuations for the path 2048 m long is explained by the fact that on these paths the turbulent atmosphere makes essential contribution to the signal fluctuations. This contention follows from the behavior of the intensity fluctuation spectra for the path 2048 m long shown in Fig. 2. As in Refs. 1–5, the measurements of the scintillation index were usually accompanied with the measurements of the fluctuation spectrum. As a result the scintillation index can be divided into the turbulent and snowfall components using the approximate expression

$$s^2 = s^2_t + s^2_s, \quad (2)$$

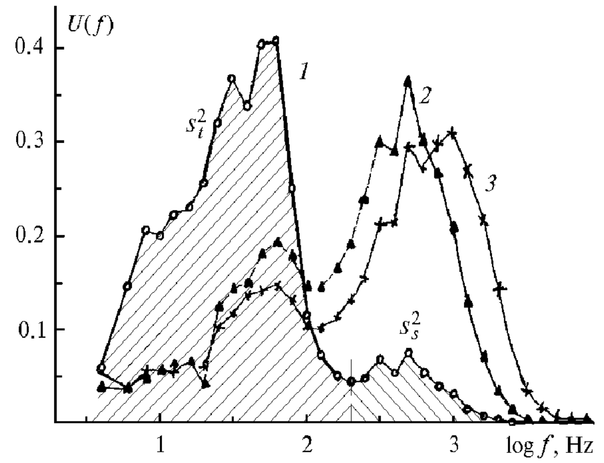

FIG. 2. Fluctuation spectra $U(f) = fW(f) / \int W(f)df$, *where* $W(f)$ *is the spectral power density at the frequency f, as fluctuations of* log *f on the path of length* z = 2048 m *for* D_{rec} = 3.1 mm: *1)* s^2 = 0.72, P = 81%, D_m = 1 mm *and* $V_\perp$ = 1 m/s; *2)* s^2 = 0.24, P = 67%, D_m = 1 mm *and* $V_\perp$ = 1 m/s; *3)* s^2 = 0.11, P = 50%, D_m = 1 mm *and* $V_\perp$ = 1.2 m/s.

where the ratio between s_t^2 and s_s^2 is specified by the corresponding ratio between the areas shown in Fig. 2.

Here, the peak near 100 Hz is caused by the turbulent atmosphere and the peak clubered at 1 kHz is caused by the snowfall. Separating the spectra in the points of the principal minima and calculating the ratio of the areas under the curve on both sides of the minimum, we divide the scintillation index (2). For vivid presentation, these areas for P = 81% are hatched in different directions. As can be seen, the contribution of the turbulent atmosphere on the path 2048 m long is significant for the small intensity of snowfall.

The spectra of signal fluctuations on the paths 780 and 520 m long are shown in Fig. 3. The influence of turbulent atmosphere on these paths was less pronounced, but optically noticeable.

Thus, to analyze the contribution of the snowfalls to the signal fluctuations we should subtract the contribution of the turbulent atmosphere. We calculated parameter s_s^2 for snowfalls for the range of transparency variations P = 50–60% for every path length shown in Fig. 1. The results of calculations are presented in Table I.

Averaging was performed over the above-indicated range of variations of the transparency P. In addition to the desired parameter s_s^2, the average optical thicknesses τ and the scintillation indexes s^2 together with their standard deviations δτ and Δs^2 are given in Table I. The number of measurements for P = 50–60% is indicated in the last row of the table.

As could be seen from Table I and Fig. 1, the signal fluctuations on the path 2048 m long for these intensities of snowfall are much less than on shorter paths. This, in essence, indicated the presence of the regime of damping fluctuations for the non-point receiver. This is the main conclution of this paper.

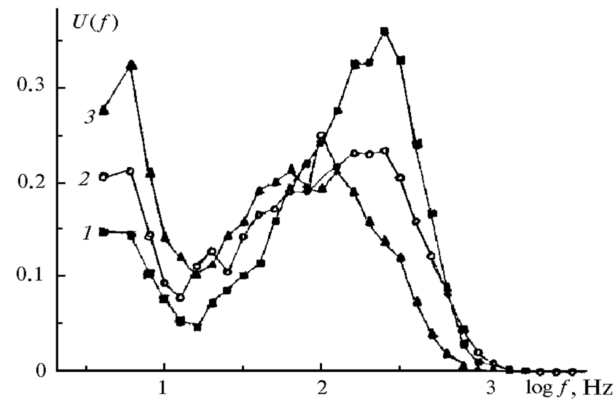

FIG. 3. Fluctuation spectra $U(f)$ *as function of* log *f on path* 520 *and* 780 m *long for* D_{rec} = 3.1 mm: *1)* s^2 = 0.38, P = 51%, D_m = 1–3 mm, $V_\perp$ = 0.2 m/s *and* L = 780 m; *2)* s^2 = 0.26, P = 55%, D_m = 1–3 mm, $V_\perp$ = 0.2 m/s *and* L = 780 m; *2)* s^2 = 0.26, P = 55%, D_m = 1–3 mm, $V_\perp$ = 3.0 m/s *and* L = 520 m; *3)* s^2 = 0.08, P = 89%, D_m = 2–3 mm, $V_\perp$ = 0.77 m/s *and* L = 520 m.

TABLE I.

L, m	τ	Δτ	s^2	Δs^2	s_s^2	N
260	0.79	0.023	0.18	0.013	0.18	119
520	1.58	0.023	0.35	0.064	0.26	136
780	2.34	0.025	0.33	0.061	0.24	50
2048	6.14	0.020	0.09	0.018	0.07	22

ACKNOWLEDGMENT

This work was supported in part by Russian Foundation of Basic Research (project 96–02–16388).

REFERENCES

1. A.F. Zhukov, Atmos. Oceanic Opt. **6**, No. 1, 19–21 (1993).
2. A.G. Borovoy, A.F. Zhukov, N.A. Vostretsov, Atmos. Oceanic Opt. **7**, No. 1, 61–62 (1994).
3. N.A. Vostretsov, A.F. Zhukov, Atmos. Oceanic Opt. **8**, No. 5, 414 (1995).
4. A.F. Zhukov, N.A. Vostretsov, Atmos. Oceanic Opt. **9**, No. 8, 670–676 (1996).
5. A.G. Borovoy, A.F. Zhukov, N.A. Vostretsov, B.A. Kargin, S.M. Prigarin, Atmos. Oceanic Opt. **10**, No. 3, 141–145 (1997).